© 2014. Published by The Company of Biologists Ltd | Development (2014) 141, 1104-1109 doi:10.1242/dev.098905

RESEARCH ARTICLE

An anterior limit of FGF/Erk signal activity marks the earliest future somite boundary in zebrafish

Ryutaro Akiyama*, Miwa Masuda‡, Shoichiro Tsuge, Yasumasa Bessho and Takaaki Matsui§

ABSTRACT

Vertebrate segments called somites are generated by periodic segmentation of the anterior extremity of the presomitic mesoderm (PSM). During somite segmentation in zebrafish, *mesp-b* determines a future somite boundary at position B-2 within the PSM. Heat-shock experiments, however, suggest that an earlier future somite boundary exists at B-5, but the molecular signature of this boundary remains unidentified. Here, we characterized fibroblast growth factor (FGF) signal activity within the PSM, and demonstrated that an anterior limit of downstream Erk activity corresponds to the future B-5 somite boundary. Moreover, the segmentation clock is required for a stepwise posterior shift of the Erk activity boundary during each segmentation. Our results provide the first molecular evidence of the future somite boundary at B-5, and we propose that clock-dependent cyclic inhibition of the FGF/Erk signal is a key mechanism in the generation of perfect repetitive structures in zebrafish development.

KEY WORDS: FGF signalling, Clock, Segmentation, Somitogenesis

INTRODUCTION

Proper formation of a well-proportioned body in multicellular organisms requires spatiotemporal control of multiple biological processes during development. For instance, the regularity of repetitive structures in vertebrate bodies is derived from the vertebrate segments called somites, which are generated by periodic segmentation of the uniform presomitic mesoderm (PSM) (Pourquié, 2001). The periodicity of segmentation is regulated by oscillation of the segmentation clock genes, and the position of segmentation is determined by a gradient of fibroblast growth factor (FGF) (Dubrulle et al., 2001; Dubrulle and Pourquié, 2004; Holley, 2007; Pourquié, 2001; Sawada et al., 2001).

The first detectable sign of a future segment boundary, as visualized by the expression of *mesoderm posterior homolog-b* (*mesp-b*; *mespba* – Zebrafish Information Network), appears at a distance of two somite lengths posterior to B0 (B-2, between S-I and S-II; see Fig. 1D for nomenclature) in the anterior PSM in zebrafish (Sawada et al., 2000), although this may not be the earliest event in boundary determination. A brief exposure of zebrafish embryos to heat shock disrupts somite segmentation after four cycles of normal segmentation (Roy et al., 1999), suggesting that the boundaries of at least five somites (from B-1 to B-5, between S-IV and S-V) are predetermined somewhere in the uniform PSM. However, no molecular sign marking the position of the future somite boundary at B-5 has yet been identified. By precise measurement of the FGF active domain and transient manipulation of FGF signal activity in zebrafish embryos, we show in this study that the anterior limit of FGF/Erk activity corresponds to the future somite boundary at B-5.

Gene Regulation Research, Nara Institute Science and Technology, 8916-5 Takayama, Nara 630-0101, Japan.
*Present address: Department of Genetics, Cell Biology and Development, University of Minnesota, Minneapolis, MN 55455, USA. ‡Present address: Laboratory for Neurobiology of Synapse, RIKEN Brain Science Institute, Saitama 351-0198, Japan.

§Author for correspondence (matsui@bs.naist.jp)

Received 11 May 2013; Accepted 15 December 2013

RESULTS

The *fgf8a* gradient moves continuously towards the posterior during somitogenesis

In chick, an *Fgf8* gradient, generated by restricted transcription and mRNA decay of *Fgf8*, is essential for setting up the position of the segmentation (Dubrulle and Pourquié, 2004). In zebrafish, segmentation defects can be seen in *ace/ace* embryos (*fgf8a* mutants) (supplementary material Fig. S1) (see also Reifers et al., 1998), suggesting that zebrafish *fgf8a* has a similar role as chick Fgf8 in the context of somitogenesis. However, it has been reported that at least three *fgfs* (*fgf4*, *fgf8a* and *fgf24*) are expressed in the tailbud region (data retrieved from the Zebrafish Information Network, http://zfin.org/, 4 April 2013), and that *fgf8a* and *fgf24* are together required to generate posterior mesoderm (Draper et al., 2003). We thus observed their expression in the tailbud of zebrafish embryos at a particular somite stage and tested whether the *fgf* gradient is seen in zebrafish embryos. Although expression of *fgf4* and *fgf24* was detected in the midline structures of the tailbud, a clear gradient of neither *fgf4* nor *fgf24* was observed in the PSM (supplementary material Fig. S2). By contrast, *fgf8a* mRNA was most abundant in a region of the posterior PSM between Kupffer's vesicle and the posterior end of the tailbud, at the 5-somite stage, and declined gradually towards the anterior (Fig. 1A). To determine how this *fgf8a* gradient moves during somite segmentation, we measured levels of *fgf8a* expression in each embryo and then compared the position of the anterior limit of the *fgf8a* gradient among several embryos, which are arranged in an order of time progression by both the somite number and PSM length as a time indicator (for details, see Materials and Methods). Although PSM length varied between embryos at the same 5-somite stage, the length of the *fgf8a* gradient between the anterior border and the posterior end remained constant (Fig. 2A,C; supplementary material Fig. S10). When a pair of new somites formed, meaning that the embryo had reached the 6-somite stage, the PSM shortened immediately by about one somite length, whereas the length of the *fgf8a* gradient did not change at the transition between the 5- and 6-somite stages or indeed throughout the 6-somite stage (Fig. 2A,C; supplementary material Fig. S10). These results suggest that the *fgf8a* gradient moves continuously towards the posterior as the tail elongates.

The *fgf8a* gradient is converted into the Erk activity boundary

Fgf8 binds to and activates Fgf receptors (Fgfrs), which then transduces the FGF signal to the Ras/Erk pathway, leading to the transcriptional activation of target genes including positive and

Development (2014) doi:10.1242/dev.098905

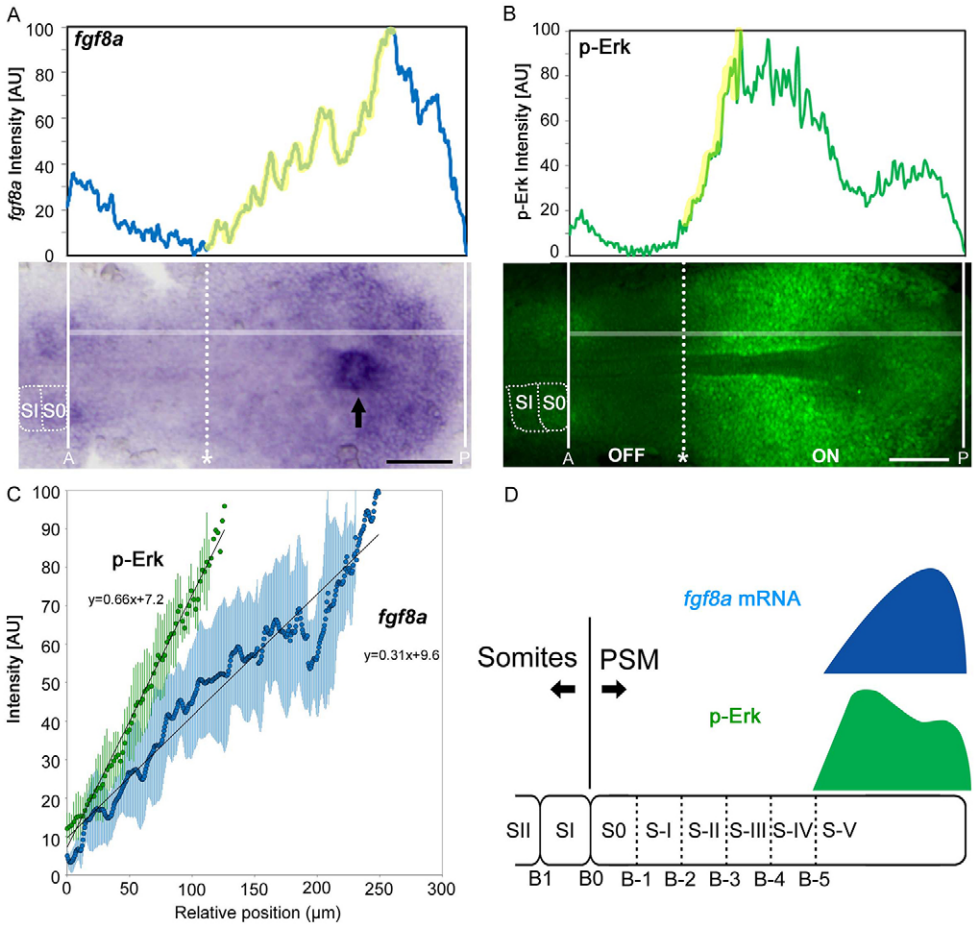

Fig. 1. *fgf8a* mRNA shows graded distribution in the PSM, whereas FGF downstream signal activity, represented by p-Erk levels, does not.
(A,B) Representative images of *fgf8a* expression (A) and p-Erk distribution (B) showing a gentle slope and a steep gradient, respectively. Signal intensities (graphs; AU, arbitrary unit) were measured by ImageJ software from the original images. Anterior and posterior ends of the PSM are marked by white lines. The position of the anterior extremity (dotted lines) was estimated by comparison of signal intensity (upper panel) and visual observation (lower panel). Dorsal view of tailbud regions in flat-mounted embryos, anterior to the left. The horizontal white lines in the lower images mark the paths along which the signal intensities shown in the upper panel were recorded. Arrow indicates Kupffer's vesicle. Scale bars: 100 μm. (C) Comparison of slopes between *fgf8a* expression and p-Erk distribution. Intensity plots of the upward slope regions of the gradients represented by the yellow line in the graphs in A and B. Approximation formulae of *fgf8a* (n=8) and p-Erk (n=7) were calculated from average values of signal intensities, respectively. Dots indicate averages and green/blue bars indicate s.d. (D) Schematic of the distribution of *fgf8a* mRNA (blue) and p-Erk (green). B, boundary; PSM, presomitic mesoderm; S, somite. Prospective somites and future somite boundaries in the PSM are numbered as described by Pourquié and Tam (Pourquié and Tam, 2001).

negative feedback regulators (Dorey and Amaya, 2010; Tsang and Dawid, 2004). The Ras/Erk pathway in *Xenopus* has the mechanistic property of generating a non-linear switch-like response, in which individual cells exhibit either 'ON' or 'OFF' status (Ferrell and Machleder, 1998; Xiong and Ferrell, 2003). In chick embryos, however, graded activation of the Erk pathway is seen in the PSM (Delfini et al., 2005), whereas in mouse embryos Erk activity displays a different dynamic state, namely an oscillatory pattern within the PSM (Niwa et al., 2007; Niwa et al., 2011). These findings suggest that the Erk pathway operates with species specificity in the PSM. To test the dynamic state of Erk activity in zebrafish PSM, we monitored the active (phosphorylated) form of Erk (p-Erk) by immunostaining using an anti-p-Erk antibody. Although the expression of *fgf8a* displayed a single peak gradient in zebrafish PSM (Fig. 1A,C), the Erk activity pattern did not (Fig. 1B,C); rather, Erk was highly activated in PSM cells located at rostral and caudal sites of Kupffer's vesicle, showing a bimodal pattern (Fig. 1B; supplementary material Fig. S3A). In the posterior PSM cells, p-Erk signal intensity in a particular PSM cell was similar to that in its neighbours (supplementary material Fig. S3D), whereas p-Erk was not detected at all in the anterior PSM cells (supplementary material Fig. S3B). Importantly, an obvious difference in the p-Erk signal intensity could be seen at the middle of the PSM (supplementary material Fig. S3C). These results suggest that, in zebrafish PSM, the mechanistic property of the Ras/Erk pathway generates either an 'ON' (activated) or an 'OFF' (inactivated) status for Erk activity, as seen in *Xenopus* (Ferrell and Machleder, 1998; Xiong and Ferrell, 2003), and thus a boundary of Erk activity is generated within the uniform PSM.

In most developmental processes, a morphogen gradient is converted into a sharp response boundary within a uniform tissue to form proper patterns. We thus compared the *fgf8a* and p-Erk gradients in different embryos and found that the p-Erk gradient was much steeper than the *fgf8a* gradient (Fig. 1C). This result is further confirmed by comparisons of the *fgf8a* and p-Erk gradients in the same embryos (supplementary material Fig. S4A-D). These results suggest that the gentle slope of *fgf8a* is converted into the steep gradient of Erk activity, leading to generation of the Erk activity boundary in the uniform PSM. In agreement with this notion, we found that the anterior limit of Erk activity displayed stepwise changes within the PSM that correlated with the spatial periodicity of somite patterning (Fig. 2B,D; supplementary material Fig. S4E,F and Figs S11, S12). Within a particular somite stage, the ON region of Erk activity elongated gradually owing to the tail elongation, whereas the length of the OFF region (distance between B-1 and the anterior limit of Erk activity; see also Fig. 1B) remained constant (Fig. 2B,D; supplementary material Fig. S4E,F). Interestingly, when a pair of new somites formed, the ON region shortened immediately by about one somite length so that the length of the OFF region was precisely maintained (Fig. 2B,D; supplementary material Fig. S4E,F). Furthermore, double staining of p-Erk and *her1* expression confirmed that the stepwise changes in the anterior limit of Erk activity were consistent with both somite number and phase propagation of *her1* oscillation (supplementary material Fig. S5). These results therefore suggest that the anterior limit of Erk activity displays stepwise movements that correlate with somite segmentation and corresponds to the future somite boundary in the uniform PSM.

Development (2014) doi:10.1242/dev.098905

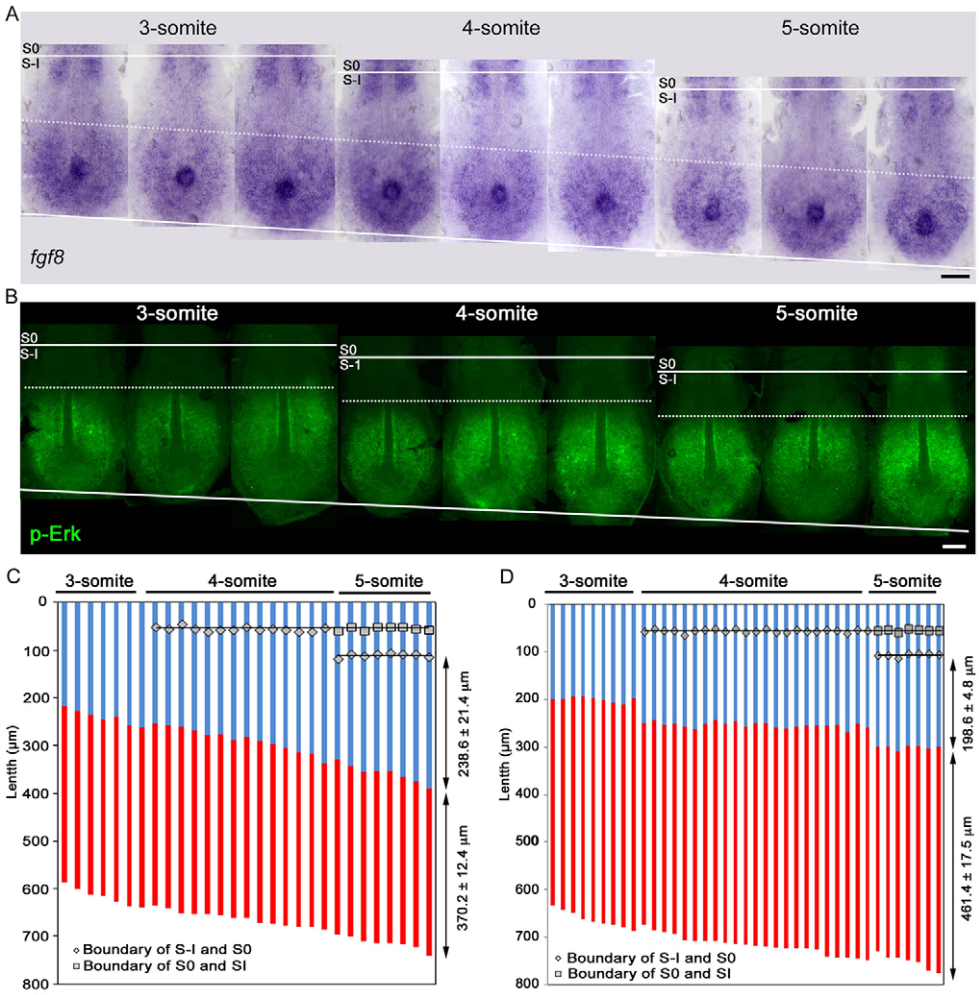

Fig. 2. A continuous pattern of *fgf8a* mRNA is converted into a stepwise pattern of p-Erk during each somite segmentation. (A) Representative images of *fgf8a* expression in the tailbud regions of embryos at the 3- to 5-somite stages. The position of the anterior extremity of *fgf8a* expression is indicated by the dotted line. (B) Representative images of p-Erk distribution in the tailbud regions of embryos at the 3- to 5-somite stages. Dorsal view of tailbud regions, anterior to the top. (C,D) Quantitative data of *fgf8a* expression (C) or p-Erk distribution (D). Embryos (C, *n*=29; D, *n*=39) were arranged in order of time progression, which was estimated by both the somite number and the PSM length. In C, red and blue stripes within each column indicate expression and non-expression domains of *fgf8a* in each embryo, respectively. Statistical significance of variation (*2P*<0.05) could be seen in *fgf8a* expression region (C.V.=0.033) versus *fgf8a* non-expression region (C.V.=0.090). In D, red and blue stripes within each column indicate ON and OFF regions of Erk activity in each embryo, respectively. Scale bars: 100 μm. Statistical significance of variation (*2P*<0.05) could be seen in the OFF region (C.V.=0.024) versus the ON region (C.V.=0.038).

The anterior limit of Erk activity represents the future somite boundary at B-5

Expression of *mesp-b* appears in the rostral parts of S-I and S-II in the anterior PSM, and is the molecular sign of the future somite boundary B-2 between S-I and S-II (Holley, 2007; Sawada et al., 2000). Double staining for p-Erk and *mesp-b* expression revealed that the anterior limit of Erk activity was not concomitant with the position at S-II where *mesp-b* is expressed (supplementary material Fig. S6). The anterior limit of Erk activity was located at a considerably more posterior site in the PSM (supplementary material Fig. S6), suggesting the possibility that the anterior limit of Erk activity marks a future somite boundary, such as B-5 between S-IV and S-V.

If this is the case, misplacement of the Erk activity boundary towards the anterior would result in an anterior shift of B-2 future somite boundary position, marked by *mesp-b* expression, leading to decreased size of the resultant somite. To test this possibility, we applied a strategy similar to that of the FGF signal perturbations reported by Sawada et al. (Sawada et al., 2001); we enhanced Erk activity for 4 minutes in embryos at the 2-somite stage using the dual-specificity phosphatase inhibitor BCI (Molina et al., 2009) (Fig. 3A). p-Erk signals were intensified immediately after BCI treatment (2-somite stage), resulting in an anterior shift (~14 μm) of the Erk activity boundary that is estimated by the difference of the OFF region length of p-Erk between embryos treated with DMSO (vehicle) and BCI (Fig. 3B,C; Table 1). However, the anterior limit of Erk activity returned to its normal position by the 3-somite stage (one round of segmentation after BCI treatment) (Fig. 3C). These results indicate that the Erk activity boundary transiently shifted towards the anterior immediately after BCI treatment.

If the Erk activity boundary represents the B-5 future somite boundary, the transient anterior shift of this boundary may alter *mesp-b* expression position towards the anterior only when three rounds of segmentation (5-somite stage) had occurred after BCI treatment. To test this possibility, we investigated the distribution of *mesp-b* expression in BCI-treated embryos. Although the anterior limit of Erk activity was shifted just after BCI treatment (Fig. 3C), *mesp-b* expression occurred normally at this time point (Fig. 3D). Only when three rounds of segmentation had occurred after BCI treatment (5-somite stage) was the width of *mesp-b* stripes shortened (~13 μm) (Fig. 3D,E; Table 1). Consistently, this manipulation eventually led to decreased size (~13 μm) of the resultant 7th somite (Fig. 3F,G; Table 1). Similar results could be obtained when 4- or 10-somite stage embryos were treated with BCI (Table 1). We also investigated whether *mesp-b* knockdown affected the distribution of the anterior limit of Erk activity. Although *mesp-b* knockdown resulted in mild disruption of the somite boundary, this manipulation did not affect the stepwise movement of the anterior limit of Erk activity seen in cycles of somite segmentation (supplementary material Fig. S7). These results therefore suggest that the anterior limit of Erk activity is the future somite boundary at B-5; this is an earlier sign of the future somite boundary than that of *mesp-b* expression at B-2.

Development (2014) doi:10.1242/dev.098905

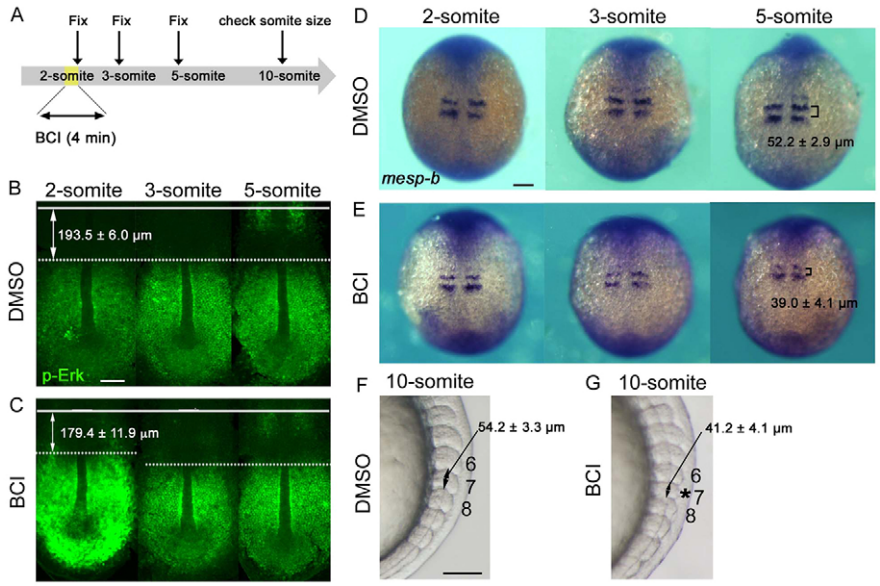

Fig. 3. The anterior limit of Erk activity marks the future somite boundary at B-5. (A) Schematic of the experimental design. (B,C) Representative images of p-Erk distribution in 2-, 3- and 5-somite-stage embryos treated with DMSO (vehicle; B) or BCI (C). The B-1 position is marked by a white line. The anterior limit of Erk activity is indicated by a white dotted line. In BCI-treated embryos, p-Erk signals were highly activated and expanded to the anterior only at the 2-somite stage (C). (D,E) Representative images of *mesp-b* expression in 2-, 3- and 5-somite stage embryos treated with DMSO (D) or BCI (E). Although p-Erk signals were altered immediately after BCI treatment (C), *mesp-b* expression changed only in S-I (brackets) of 5-somite stage embryos, which would generate a smaller 7th somite as shown in G. (F,G) Representative images of 10-somite-stage embryos treated with DMSO (F) or BCI (G). BSI treatment at the 2-somite stage led to decreased size of 7th somite (G). Scale bars: 100 μm.

Time-lapse imaging followed by p-Erk staining revealed that the position of the anterior limit of Erk activity was maintained in several cycles of somite segmentation (supplementary material Fig. S8A). We thus reasoned that targeted cell fluorescence labelling and time-lapse imaging could confirm whether this position represents the future somite boundary at B-5. To test this possibility, we photo-converted cells at the presumptive p-Erk boundary in *Tg[her1:KikGR]* embryos and traced the trajectory of the cells (supplementary material Fig. S8B and Movie 1). Although the alignment of the photo-converted cells (supplementary material Fig. S8B, red cells) changed during somitogenesis, a proportion of the cells finally resided at the rostral end of the somite when five rounds of segmentation had completed, meaning that the position adjacent to the photo-converted cells (supplementary material Fig. S8B, red arrowhead) corresponds to the future somite boundary at B-5 (see also Fig. 1D).

Somite segmentation clock controls the stepwise movement of the Erk activity boundary during somitogenesis

Because the repetitive structure of somites is generated from the temporal periodicity created by the somite segmentation clock (Oates et al., 2012; Pourquié, 2011), we hypothesized that proper functioning of the segmentation clock is required for the stepwise movement of the future somite boundary. To test this possibility, we disrupted the segmentation clock in zebrafish embryos by knocking down two segmentation clock genes, *her1* and *her7*, and investigated the dynamics of the anterior limit of Erk activity in the manipulated embryos. As shown previously (Henry et al., 2002), double knockdown of *her1* and *her7* resulted in the loss of metameric structures of somites (supplementary material Fig. S9B). Erk activation occurred normally even in the manipulated embryos (supplementary material Fig. S9C,D). However, the anterior limit of Erk activity lost its stepwise pattern in each cycle of somite segmentation (Fig. 4A,B; supplementary material Fig. S13). These results therefore suggest that the segmentation clock is required for the stepwise movement of the anterior limit of Erk activity in the PSM (Fig. 4C).

DISCUSSION

In a clock and wavefront model, the clock controls when the somite boundaries form and the wavefront determines where they form (Cooke and Zeeman, 1976). It has been proposed that, in zebrafish, Her1 homodimer- and Her7:Hes6 heterodimer-based negative feedback loops constitute the clock, and FGF gradients constitute

Table 1. Effects of BCI on somite segmentation

	Length of region			
	n	DMSO	*n*	BCI
2-somite stage				
p-Erk OFF region (2s)	18	193.5±6.0	13	179.4±11.9*
mesp-b (5s)	16	52.2±2.9	17	39.0±4.1*
Somite (7s)	17	54.2±3.3	19	41.2±4.1*
4-somite stage				
p-Erk OFF region (4s)	8	193.9±7.6	7	179.6±12.1*
mesp-b (7s)	8	51.6±3.7	8	35.9±6.8*
Somite (9s)	10	56.4±3.6	9	40.9±3.1*
10-somite stage				
p-Erk OFF region (10s)	12	201.1±2.0	16	172.6±5.8*
mesp-b (13s)	20	51.0±3.1	21	41.1±3.9*
Somite (15s)	22	53.1±2.7	20	43.0±2.8*

Statistically significant difference (*P<0.05) could be seen in DMSO- versus BCI-treated embryos.
s, somite.

Development (2014) doi:10.1242/dev.098905

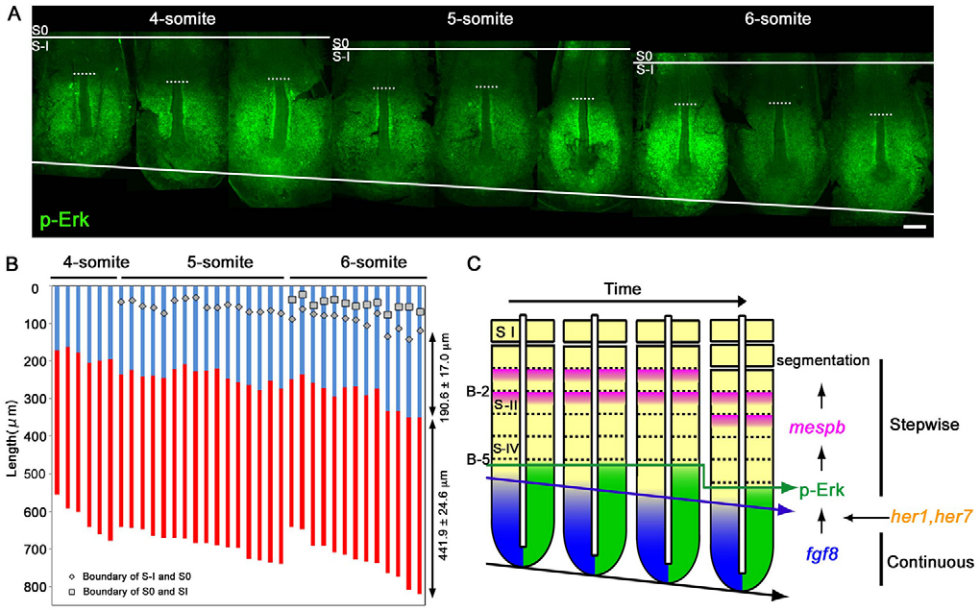

Fig. 4. Double knockdown of *her1* and *her7* leads to loss of stepwise p-Erk pattern during somite segmentation. (A) Representative images of p-Erk distribution in embryos at the 4- to 6-somite stages. Dorsal view of the tailbud region, anterior to the top. Scale bar: 100 μm. (B) Quantitative data of p-Erk distribution in *her1* and *her7* morphants (*n*=35). Red and blue stripes within each column indicate ON and OFF regions, respectively, of p-Erk activity in each embryo. Statistical significance of variation (*2P*>0.05) could not be seen in the OFF region (C.V.=0.089) versus the ON region (C.V.=0.056). (C) Generation of the future somite boundary at B-5. The *fgf8a* mRNA gradient progresses continuously towards the posterior at the same rate as elongation of the PSM, whereas the activity of p-Erk, downstream of FGF signalling, exhibits a stepwise pattern during each somite segmentation. This pattern is generated by a mechanism depending on the somite segmentation clock in zebrafish. The anterior limit of Erk activity represents the positioning of the future somite boundary at B-5; p-Erk is therefore an earlier molecular marker of the future somite boundary than *mesp-b*, a determinant of the future somite boundary at B-2.

the wavefront (Holley, 2007; Pourquié, 2001; Schröter et al., 2012; Trofka et al., 2012). In this study, we provide additional information for the mechanism underlying zebrafish somitogenesis. Because the single peak *fgf8a* gradient moved continuously towards the posterior (Fig. 2A,C; supplementary material Fig. S4E,F), the *fgf8a* gradient acts as a steadily regressing wavefront. As the *fgf8a* gradient is converted into the Erk activity boundary (Fig. 1; supplementary material Figs S3, S4), which corresponds to the future B-5 somite boundary (Fig. 3; supplementary material Fig. S8B and Movie 1), and because the clock regulates the stepwise movements of the future somite boundary (Fig. 4; supplementary material Fig. S9), the anterior limit of Erk activity represents a 'signal integration spot' of the clock and the wavefront.

In mouse, the clock (Notch oscillators such as Hes7 and Lfng) controls oscillation of Erk activity, and Erk oscillation periodically allows Notch signals to induce *Mesp2* expression at S-I, suggesting that Erk oscillation represents a rippled wavefront (Niwa et al., 2011). These findings suggest that, although the detailed mechanisms are different, there is a common logic of somitogenesis in zebrafish and mouse: Notch oscillators periodically modulate the FGF/Erk wavefront at the signal integration spot to regulate spatiotemporal periodicity. In chick, although Erk activity declines gradually towards the anterior (Delfini et al., 2005), whether the gradient of Erk activity corresponds to a future somite boundary and whether the gradient shows an oscillatory pattern remain unknown. Therefore, it would be of great interest to understand a common and/or specific logic of somitogenesis in vertebrates by comparing regulatory mechanisms of somite formation in such different species.

Conclusion

Pattern formation is one of the most important processes of vertebrate morphogenesis. In the case of somites, pre-patterning over a distance of about five somites is thought to be determined within apparently uniform tissue composed of somite progenitor cells. Using somitogenesis as a model to investigate how patterns are generated during development, we reveal that a morphogen gradient is converted into a sharp response boundary of intracellular signalling, providing positional information as a future segment boundary, and that clock-dependent stepwise movement of this sharp response boundary is required to generate the perfect metameric pattern of the vertebrate body during development.

MATERIALS AND METHODS

Zebrafish

Wild-type and ace^{ti282a} (*fgf8a* mutant) zebrafish were used in this study. As described previously (Matsui et al., 2011), substitution from G to A in the *ace* allele was detected by sequence analyses of the DNA fragment obtained from each embryo after *in situ* hybridization or immunohistochemistry.

Whole-mount *in situ* hybridization and immunohistochemistry

Whole-mount *in situ* hybridization and immunohistochemistry were performed as described previously (Matsui et al., 2005; Matsui et al., 2011). cDNA fragments of *fgf8a*, *mesp-b* and *her1* were used as templates for antisense probes.

Morpholinos (MOs) and injection

The following antisense MO oligonucleotides against *her1*, *her7* and *mesp-b* and a control MO were obtained from Gene Tools: control-MO: 5′-CCTCTTACCTCAGTTACAATTTATA-3′; *her1*-MO: 5′-TTCGACTT-GCCATTTTTGGAGTAAC-3′ (Henry et al., 2002); *her7*-MO: 5′-CAGTCTGTGCCAGGATTTTCATTGC-3′ (Henry et al., 2002); *mesp-b*-MO: 5′-TCGGTTCTTGCTTGAGGTTTGCATG-3′ (Lee et al., 2009). *her1*-MO plus *her7*-MO (6.25 ng each), *mesp-b*-MO (5 ng) or control-MO (12.5 ng or 5 ng) were injected into the yolk of one-cell-stage zebrafish embryos

as described previously (Matsui et al., 2011). Injected embryos were collected and fixed at the indicated time points, and then used for experiments including *in situ* hybridization and immunohistochemistry.

Transient treatment of BCI

Embryos were obtained by mating wild-type fish and were cultured normally until 10.5-11 hours post-fertilization (hpf). Embryos at the 2-somite stage were treated with 0.1 mg/ml BCI (Dual Specificity Protein Phosphatase 1/6 Inhibitor, Calbiochem) for 4 minutes, and then washed extensively with embryo medium. Embryos were fixed just after treatment (2-somite stage), or after one (3-somite stage), three (5-somite stage) or eight (10-somite stage) rounds of segmentation following BCI treatment.

Graphical analyses

The embryos were flat-mounted in Vectashield mounting medium, which contains propidium iodide (PI) (Vector Laboratories). Immunofluorescence signals were visualized and photographed using an LSM510-META or LSM710 confocal microscope (Zeiss). Sequential confocal images were stacked. The position of the somite boundary and posterior end of the PSM was estimated by visual observation of PI staining in combination with bright-field microscopy. Embryos were grouped according to somite number, and were arranged in order of PSM length, because the PSM gradually elongates along with tail elongation. Signal intensity was measured by using ImageJ software (National Institutes of Health), and background was subtracted to remove any tissue autofluorescence from the signal. The position of the anterior limit of *fgf* expression and the Erk activity was determined by the comparison between visual observation and signal intensity plot.

Statistical analyses

The coefficient of variation (C.V.) was calculated by the ratio of the s.d. to the mean. Differences in variances and means were analysed by one-tailed F test of equality of variance and two-tailed Welch's *t*-test, respectively. Results in the F test and *t*-test were considered significant when $2P<0.05$ and $P<0.05$, respectively.

Time-lapse imaging

In order to label PSM cells with a photo-convertible fluorescent protein named KikGR, we generated a transgenic line *Tg[her1:KikGR]* using the Tol2 system (Kawakami et al., 2004; Urasaki et al., 2006). *Tg[her1:KikGR]* carries the zebrafish *her1* promoter, *KikGR* full length cDNA (MBL), nuclear localization signal sequence and SV40 poly A sequence. A 405 nm laser was used in photo-conversion of KikGR. Time-lapse image acquisition was performed by using Olympus FV-1000-D confocal microscope and FLUOVIEW software.

Acknowledgements

We are grateful to Shinji Takada for helpful discussions and critical reading of the manuscript. We also thank Ian Smith, Wong Kah Loon and Fiqri Dizar Khaidizar for help in preparing the manuscript; Maiko Yokouchi, Hiroko Shigesato, Tatsuro Matta, Hiroshi Okamoto and Ryosuke Tatsumi for technical assistance.

Competing interests

The authors declare no competing financial interests.

Author contributions

R.A. performed the experiments and data analysis. M.M. and S.T. performed the experiments. Y.B. contributed to experimental design. T.M. designed and performed the experiments, analysed the data and wrote the manuscript.

Funding

This work was supported by Grants-in-Aid for Scientific Research (B), Grants-in-Aid for Scientific Research on Innovative Areas, and Grant-in-Aid for Young Scientists (A) from the Ministry of Education, Culture, Sports, Science and Technology (MEXT), Japan.

Supplementary material

Supplementary material available online at
http://dev.biologists.org/lookup/suppl/doi:10.1242/dev.098905/-/DC1

References

Cooke, J. and Zeeman, E. C. (1976). A clock and wavefront model for control of the number of repeated structures during animal morphogenesis. *J. Theor. Biol.* **58**, 455-476.

Delfini, M. C., Dubrulle, J., Malapert, P., Chal, J. and Pourquié, O. (2005). Control of the segmentation process by graded MAPK/ERK activation in the chick embryo. *Proc. Natl. Acad. Sci. USA* **102**, 11343-11348.

Dorey, K. and Amaya, E. (2010). FGF signalling: diverse roles during early vertebrate embryogenesis. *Development* **137**, 3731-3742.

Draper, B. W., Stock, D. W. and Kimmel, C. B. (2003). Zebrafish fgf24 functions with fgf8 to promote posterior mesodermal development. *Development* **130**, 4639-4654.

Dubrulle, J. and Pourquié, O. (2004). fgf8 mRNA decay establishes a gradient that couples axial elongation to patterning in the vertebrate embryo. *Nature* **427**, 419-422.

Dubrulle, J., McGrew, M. J. and Pourquié, O. (2001). FGF signaling controls somite boundary position and regulates segmentation clock control of spatiotemporal Hox gene activation. *Cell* **106**, 219-232.

Ferrell, J. E., Jr and Machleder, E. M. (1998). The biochemical basis of an all-or-none cell fate switch in Xenopus oocytes. *Science* **280**, 895-898.

Henry, C. A., Urban, M. K., Dill, K. K., Merlie, J. P., Page, M. F., Kimmel, C. B. and Amacher, S. L. (2002). Two linked hairy/Enhancer of split-related zebrafish genes, her1 and her7, function together to refine alternating somite boundaries. *Development* **129**, 3693-3704.

Holley, S. A. (2007). The genetics and embryology of zebrafish metamerism. *Dev. Dyn.* **236**, 1422-1449.

Kawakami, K., Takeda, H., Kawakami, N., Kobayashi, M., Matsuda, N. and Mishina, M. (2004). A transposon-mediated gene trap approach identifies developmentally regulated genes in zebrafish. *Dev. Cell* **7**, 133-144.

Lee, H. C., Tseng, W. A., Lo, F. Y., Liu, T. M. and Tsai, H. J. (2009). FoxD5 mediates anterior-posterior polarity through upstream modulator Fgf signaling during zebrafish somitogenesis. *Dev. Biol.* **336**, 232-245.

Matsui, T., Raya, A., Kawakami, Y., Callol-Massot, C., Capdevila, J., Rodríguez-Esteban, C. and Izpisúa Belmonte, J. C. (2005). Noncanonical Wnt signaling regulates midline convergence of organ primordia during zebrafish development. *Genes Dev.* **19**, 164-175.

Matsui, T., Thitamadee, S., Murata, T., Kakinuma, H., Nabetani, T., Hirabayashi, Y., Hirate, Y., Okamoto, H. and Bessho, Y. (2011). Canopy1, a positive feedback regulator of FGF signaling, controls progenitor cell clustering during Kupffer's vesicle organogenesis. *Proc. Natl. Acad. Sci. USA* **108**, 9881-9886.

Molina, G., Vogt, A., Bakan, A., Dai, W., Queiroz de Oliveira, P., Znosko, W., Smithgall, T. E., Bahar, I., Lazo, J. S., Day, B. W. et al. (2009). Zebrafish chemical screening reveals an inhibitor of Dusp6 that expands cardiac cell lineages. *Nat. Chem. Biol.* **5**, 680-687.

Niwa, Y., Masamizu, Y., Liu, T., Nakayama, R., Deng, C. X. and Kageyama, R. (2007). The initiation and propagation of Hes7 oscillation are cooperatively regulated by Fgf and notch signaling in the somite segmentation clock. *Dev. Cell* **13**, 298-304.

Niwa, Y., Shimojo, H., Isomura, A., González, A., Miyachi, H. and Kageyama, R. (2011). Different types of oscillations in Notch and Fgf signaling regulate the spatiotemporal periodicity of somitogenesis. *Genes Dev.* **25**, 1115-1120.

Oates, A. C., Morelli, L. G. and Ares, S. (2012). Patterning embryos with oscillations: structure, function and dynamics of the vertebrate segmentation clock. *Development* **139**, 625-639.

Pourquié, O. (2001). Vertebrate somitogenesis. *Annu. Rev. Cell Dev. Biol.* **17**, 311-350.

Pourquié, O. (2011). Vertebrate segmentation: from cyclic gene networks to scoliosis. *Cell* **145**, 650-663.

Pourquié, O. and Tam, P. P. (2001). A nomenclature for prospective somites and phases of cyclic gene expression in the presomitic mesoderm. *Dev. Cell* **1**, 619-620.

Reifers, F., Böhli, H., Walsh, E. C., Crossley, P. H., Stainier, D. Y. and Brand, M. (1998). Fgf8 is mutated in zebrafish acerebellar (ace) mutants and is required for maintenance of midbrain-hindbrain boundary development and somitogenesis. *Development* **125**, 2381-2395.

Roy, M. N., Prince, V. E. and Ho, R. K. (1999). Heat shock produces periodic somitic disturbances in the zebrafish embryo. *Mech. Dev.* **85**, 27-34.

Sawada, A., Fritz, A., Jiang, Y. J., Yamamoto, A., Yamasu, K., Kuroiwa, A., Saga, Y. and Takeda, H. (2000). Zebrafish Mesp family genes, mesp-a and mesp-b are segmentally expressed in the presomitic mesoderm, and Mesp-b confers the anterior identity to the developing somites. *Development* **127**, 1691-1702.

Sawada, A., Shinya, M., Jiang, Y. J., Kawakami, A., Kuroiwa, A. and Takeda, H. (2001). Fgf/MAPK signalling is a crucial positional cue in somite boundary formation. *Development* **128**, 4873-4880.

Schröter, C., Ares, S., Morelli, L. G., Isakova, A., Hens, K., Soroldoni, D., Gajewski, M., Jülicher, F., Maerkl, S. J., Deplancke, B. et al. (2012). Topology and dynamics of the zebrafish segmentation clock core circuit. *PLoS Biol.* **10**, e1001364.

Trofka, A., Schwendinger-Schreck, J., Brend, T., Pontius, W., Emonet, T. and Holley, S. A. (2012). The Her7 node modulates the network topology of the zebrafish segmentation clock via sequestration of the Hes6 hub. *Development* **139**, 940-947.

Tsang, M. and Dawid, I. B. (2004). Promotion and attenuation of FGF signaling through the Ras-MAPK pathway. *Sci. STKE* **2004**, pe17.

Urasaki, A., Morvan, G. and Kawakami, K. (2006). Functional dissection of the Tol2 transposable element identified the minimal cis-sequence and a highly repetitive sequence in the subterminal region essential for transposition. *Genetics* **174**, 639-649.

Xiong, W. and Ferrell, J. E., Jr (2003). A positive-feedback-based bistable 'memory module' that governs a cell fate decision. *Nature* **426**, 460-465.